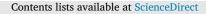
ELSEVIER



Optics Communications



journal homepage: www.elsevier.com/locate/optcom

Transport of energy through the focal region of a high-numerical-aperture system with efficient annular focusing of light beam and its optimum thin-film linear-to-radial polarization conversion



Andrey G. Sedukhin

Institute of Automation and Electrometry, Russian Academy of Sciences, Prospekt Akademika Koptyuga 1, Novosibirsk 630090, Russia

ARTICLE INFO

Keywords: Tight focusing Thin-film polarization conversion Spatial filtering Energy transfer Poynting vector Orbital angular momentum

ABSTRACT

In a previous paper [Opt. Commun. 407 (2018) 217–226], there was proposed a light-efficient, high-numericalaperture focusing system which is based on a monolithic assembly of an axicon and an inclined parabolic annular reflector (AXIPAR) optimally matched to thin-film linear-to radial polarization conversion of the illuminating beam. Also, there were derived integral expressions for the Poynting vector components of the respective, tightly focused beams having a near longitudinal polarization along the optical axis. In the present paper, being a direct continuation of the previous one, these expressions are used to analyze numerically a very specific behavior of the Poynting vector magnitude and the energy flow trajectories of deep UV laser beams in the focal regions localized in an immersion liquid. In particular, it is demonstrated graphically that, in the case of an incomplete suppression of the azimuthal component of the beams, their energy flow trajectories will have not only a small waviness near the focus, but also a moderate twisting around the optical axis, carrying an orbital angular momentum. The spatial frequency filtering of the beams is found to increase the axial size of the focal region where a more pronounced twisting is observed.

1. Introduction

The problem of maximum possible shrinkage of the transverse size of tightly focused laser beams is known to be of great importance in superresolution confocal microscopy, optical trapping, direct laser writing, and in other applications. In recent decades, there has been made a significant progress on this subject, of which prominent milestones were the use of spatial filtering of the wave components of the beams and the use of new transversely nonuniform kinds of polarization of these components. In particular, this concerns the application of annular and donut-like apertures [1-5], optimized Toraldo filters [6-9], and linear-to-radial polarization converters [10–14]. However, in practice, apart from the transverse size of the beams, there are also a number of other factors that may be significant in estimating the features of a tightly focused electromagnetic field inherent in a specific generating system. For example, it is sometimes useful to know the information on the spatial transporting of the electromagnetic energy through the focal region. This is attained by the knowledge of the behavior of the Poynting vector in the focal region, and such subject has been touched in many publications.

In particular, in Ref. [15], there have been analyzed the graphical diagrams showing the energy flow trajectories (otherwise called the

https://doi.org/10.1016/j.optcom.2018.04.078

Received 6 March 2018; Received in revised form 27 April 2018; Accepted 30 April 2018 0030-4018/© 2018 Elsevier B.V. All rights reserved.

light rays) and the contours of constant magnitude of the time-averaged Poynting vector in the focal region of a high-numerical-aperture aplanatic system illuminated by a linearly polarized plane wave. Similar diagrams were analyzed also in Ref. [7], but as applied to the focal region of a more complicated aplanatic system with a higher numerical aperture. The last system was illuminated by the first-order radially polarized Bessel-Gaussian beam, with additional filtering of this beam by a binary-phase diffractive optical element. In both cases, it was demonstrated that, in the focal volumes, the energy flow trajectories lie in the meridional planes and take mainly the form of unlimited flat concave curves. However, some trajectories may have the vortex nature and take the form of flat closed lines encompassing singular phase points. Interestingly that there are observed both forward and backward energy flows around these points. A typical behavior of the Poynting vector trajectories was analyzed also in Refs. [16] and [17] for the focal volumes of other kinds of beams-namely, for the hollow vortex scalar beams referred to as the Laguerre-Gaussian and Bessel beams. It was shown that such trajectories are no longer flat curves, but they are twisted around the optical axes, giving rise to some orbital angular momentum of the beams. These trajectories are found to be spiraling curves winding on cylinders for the Bessel beams and on hyperboloidal surfaces for the Laguerre-Gaussian beams.

E-mail address: sedukhin@iae.nsk.su.

In an attempt to integrate the main optical procedures required for the subwavelength, rotationally symmetric focusing of a laser beam, in our recent work [18], we have proposed a novel approach combining a prior efficient annular shaping of a laser beam and such subsequent procedures as its spatial frequency filtering, thin-film linear-to-radial polarization conversion, and tight reflective annular focusing. A numerical simulation for the distributions of the Poynting vector magnitude, as well as those of the electric and magnetic energy densities was also given for the far-field focal region of typical optical systems. As was demonstrated, the beams generated by such systems may possess the property of a near nondiffracting propagation in the focal region and subwavelength resolutions approaching closely the scalar diffractionlimited value. Even with no filtering, the obtained transverse resolution was found to be slightly better than those of an equivalent annularaperture aplanatic lens and an annular-aperture parabolic reflector. This may be attributed to the effect of narrowing an effective annular size of the apodization function inherent in the proposed focusing systems. As a result, one can argue that, by their performance, the proposed systems might be more preferable for some applications. Moreover, it should be recalled that such systems can easily be implemented with the help of optical components capable of operating in the deep UV spectral region and having an enhanced light efficiency, a high radiation resistance, and a wide spectral transmittance. For the most part, these factors are important, e.g., in high power laser systems.

On the other hand, one may expect that the presence of even a weak residual azimuthally polarized component of the generated beams (due to the non-ideal performance of a thin-film polarizer) under their ultra tight focusing will lead not only to interference effects and a modification of the electric and magnetic energy densities near the focus, but also to specific variations of the energy flow trajectories and the wavefronts defined by these trajectories. It is of physical and practical interest to compare the detailed phase structure of such focused fields with the fields of other focusing systems. Also, to unravel the mechanism of transporting electromagnetic energy near the focus of the systems involved and to better understand the properties of superresolution and nondiffracting propagation manifested in this region, it would be desirable to analyze the energy characteristics defined by the Poynting vector. With this object in view, in the present paper, we extend the numerical analysis carried out in Ref. [18] and study in detail the spatial variations of the Poynting vector magnitude, the behavior of the energy flow trajectories, and the respective wavefront variations in the neighborhood of the focus of the systems involved. The case of spatial frequency filtering of a focused beam is compared with the case with no filtering. Also, the focusing patterns composed of the grids of the energy flow trajectories and the wavefront profiles of the energy flow are studied in detail for important limiting cases inherent in systems with an ideal thin-film linear-to-radial polarizer.

2. Optical system and a solution for the Poynting vector

A light-efficient, tightly focusing, radially symmetric optical system we will study has been described in Ref. [18] and is given here in Fig. 1 with a part of the design parameters. We recall that this system is easily capable of performing both linear-to-radial polarization conversion and tight annular focusing of the incident laser beam in the immersion liquid (IL). It is composed of a quarter-wave plate (QWP), a diffractive optical element (DOE), and such key element as a monolithic assembly referred to as AXIPAR and combining a glass axicon (AX) and an inclined parabolic annular reflector (IPAR) in the form of a glass segment. The QWP converts the linearly polarized, collimated input beam into a circularly polarized one, while the DOE performs both the suppression of the vortex phase component of the circularly polarized beam (in the azimuthal direction ψ) and a prescribed spatial filtration of the beam (in the radial direction r). In the simplest case, for the system with no filter, the structure of the DOE corresponds to a standard spiral phase plate, with the phase retardation varying linearly in the azimuthal direction, but being uniform in the radial direction. For the system with a radial-phase-jump filter, the structure of the DOE is subdivided into two concentric circular zones-an inner circular zone and an outer annular one demarcated at a radius $r_{jump}^{(pos)}$. Within both zones, the structure of the DOE again reproduces the forms of the standard spiral phase plates, with the same strength and direction of helicity. However, the relative phase retardation at any fixed azimuthal position of the zones is changed abruptly at radius $r_{jump}^{(pos)}$ by π radians. The AXIPAR serves for the first meridional bending of the incoming beam at an angle α and the generation of a diverging conical beam, for the thin-film selection of a useful radially polarized component of the beam, and for the second steep meridional bending of the beam in such a way that the above diverging conical beam is transformed into an annular spherical beam. The conical surface of the axicon is coated with a specially designed multilayer dielectric stack, which plays the role of an obliquely illuminated thin-film polarizer (TFP) suppressing the azimuthally polarized wave components of a beam behind the OWP and the DOE (only one version of TFP's disposition is shown). A particular performance of such polarizer was given in Fig. 5 of Ref. [18]. The working surface of the IPAR is generated by the rotation of an inclined parabola, with its own axis z_{par} and the focus F, about the optical axis zat the angle α . To avoid extra phase shifts at the reflection of light from this surface (due to operation at the angles of reflection close to the angle of total internal reflection), one can deposit onto it a highly reflective coating (RC). Notice that the inclined parabolic surface of the AXIPAR (with a generating parabola inclined at the angle α to the optical axis) serves to provide an optimum operation of the TFP at constant angles $\alpha^{(i)}$ and α and is only valid for the assumed case of $n_1 = n_f$. Otherwise, it must be curved properly.

In order to conveniently calculate the sought-for energy and phase characteristics in an arbitrary point $\mathcal{P}(x, y, z)$ closed to the focus *F* of the system involved, we now write down a full vectorial solution for the time-averaged Poynting vector $\langle \mathbf{S}_{\pm} \rangle$. To this end, we combine and rewrite Eqs. (44), (46), (40), (41), (24), (26), (28), (18), (8) given in Ref. [18]:

$$\left\langle S_{\rho}\right\rangle = Q\left(\mathcal{T}_{p}+\mathcal{T}_{s}\right)\operatorname{Im}\left[I_{0}^{\prime}\left(I_{1}^{\prime\prime}\right)^{*}\right],\tag{2a}$$

$$\langle S_{\psi} \rangle = 2Q \sqrt{\mathcal{T}_{\rho} \mathcal{T}_{s}} \operatorname{Re} \left[I_{0}^{\prime} (I_{1}^{\prime})^{*} \right],$$
 (2b)

$$\langle S_z \rangle = Q\left(\mathcal{T}_p + \mathcal{T}_s\right) \operatorname{Re}\left[I_1'\left(I_1''\right)^*\right],\tag{2c}$$

$$Q = 2n_f^2 n_0 / \left(\mu_f \mu_0 c\right) \left(\pi E_0 f / \lambda_w\right)^2,$$
(3)

$$I_{0}' = \int_{\theta_{\rm inn}}^{\theta_{\rm out}} \widetilde{A}^{(f)}(\theta) \sin 2(\theta) J_{0} \left[k_{w} n_{f} \rho \sin(\theta) \right] \exp \left[i k_{w} n_{f} z \cos(\theta) \right] d\theta, \quad (4a)$$
$$I_{1}' = \int_{\theta}^{\theta_{\rm out}} \widetilde{A}^{(f)}(\theta) \sin(\theta) \cos(\theta)$$

$$< J_1 \left[k_w n_f \rho \sin(\theta) \right] \exp \left[i k_w n_f z \cos(\theta) \right] d\theta,$$
(4b)

$$I_1'' = \int_{\theta_{\rm inn}}^{\theta_{\rm out}} \widetilde{A}^{(f)}(\theta) \sin(\theta) J_1\left[k_w n_f \rho \sin(\theta)\right] \exp\left[ik_w n_f z \cos(\theta)\right] d\theta, \quad (4c)$$

$$\widetilde{A}^{(f)}(\theta) = A_0^{(i)} \left[r^{(\text{pos})}(\theta) \right] T_{\text{TOR}} \left[r^{(\text{pos})}(\theta) \right] l_{\text{AXIPAR}}^{(\text{pos})}(\theta),$$
(5)

$$A_0^{(i)} \left[r^{(\text{pos})}(\theta) \right] = \exp\left\{ - \left[r^{(\text{pos})}(\theta) \right]^2 / w_0^2 \right\},$$
(6)

$$r^{(\text{pos})}(\theta) = \frac{R_0 \left[1 + \sin(\alpha)\right]}{\left\{\cos(\alpha) + \sin(\alpha)\tan\left[\alpha^{(i)}\right]\right\}} \left[\frac{1}{\tan\left[\left(\alpha + \theta_{\text{inn}}\right)/2\right]} - \frac{1}{\tan\left[\left(\alpha + \theta\right)/2\right]}\right],$$
(7)

Download English Version:

https://daneshyari.com/en/article/7924905

Download Persian Version:

https://daneshyari.com/article/7924905

Daneshyari.com